# Structural Evolution of Multilayered, Crystalline−Amorphous Diblock Copolymer Thin Films

**Sheng Hong, William J. MacKnight, Thomas P. Russell,* and Samuel P. Gido***

*Polymer Science and Engineering Department, Materials Research Science and Engineering Center, W. M. Keck Electron Microscopy Laboratory, University of Massachusetts, Amherst, Massachusetts 01003*

*Received November 28, 2000; Revised Manuscript Received February 1, 2001*

ABSTRACT: The evolution of the morphology of a crystalline/amorphous diblock copolymer poly(ethylene oxide-*b*-1,4 butadiene) (P(EO-*b*-BD)) upon crystallization in thin films was studied via interference optical microscopy. Two-dimensional crystallization confined within the PEO lamellar layers was observed with retention of the microphase-separated lamellar morphology formed in the melt state. The morphology was further characterized by TEM and electron diffraction which showed it to consist of alternating layers of PEO and PBD with PEO crystalline chains oriented perpendicular to the lamellar layers of the microphase-separated structure. Multiple parallel layers of crystalline PEO were found by electron diffraction to be in *orientational registry* even though they were separated by approximately 10 nm thick layers of amorphous PBD.

## Introduction

The morphology of crystalline/amorphous block copolymers has attracted considerable attention recently. Studies on these materials have the potential to shed light on the fundamental physics of polymer crystallization, in general, as well as on crystallization in confined geometry. Theoretical predictions concerning the morphology of semicrystalline diblock copolymers have been developed by DiMarzio and co-workers,[1] Whitmore and Noolandi,[2] and Vilgis and Halperin[3] assuming that a thermodynamic equilibrium state can be achieved. As shown in Figure 1, this model assumes a structure of alternating crystalline and amorphous layers. In the crystalline layers there is regular chain folding with the chain stems oriented perpendicular to the interface with the amorphous domains.

Many diblock copolymer systems with a crystallizable block have been investigated. Crystallizable blocks including poly(ethylene),[4−13] poly(ethylene oxide),[14−20] poly($\epsilon$-caprolactone),[21] and poly(tetrahydrofuran)[22,23] have been studied. The amorphous blocks investigated vary considerably in terms of their glass transition temperatures and segregation interactions with the crystallizable block. The earliest work on PEO and polystyrene diblock copolymers was done by Lotz and Kovacs[24,25] in 1966, where the crystalline structure of PEO was investigated by solution grown diblock copolymer single crystals. The morphology of P(EO-*b*-S) diblock copolymers as a function of the concentration of preferential solvent was investigated by Gervais and Gallot in the 1970s.[15,26] Hamley, Ryan, and co-workers recently studied the morphology and crystallization kinetics of a series of P(EO-*b*-BO) (poly(butylene oxide)) and P(EO-*b*-PO) (poly(propylene oxide)) diblock copolymers.[6,16,27,28] More recently, the effect of ODT on bulk morphology of P(EO-*b*-S) and crystalline orientation were studied by Cheng and co-workers.[19,20]

In many of these previous studies, the final morphology was found to be path-dependent. When crystallizing the sample from a microphase-separated melt state, one of two results is obtained: (1) The microphase-separated morphology is maintained, and the crystallizable block crystallizes within the volume defined by the block copolymer microphase-separated morphology. (2) Crystallization destroys the microphase-separated morphology, and a spherulitic texture formed. The morphology of the crystalline/amorphous block copolymers was found to be heavily influenced by kinetics, similar to the case of crystallizable homopolymers. The crystalline chain orientation within the microphase-separated microdomains was also found to vary depending upon the diblock systems and the crystallization conditions.

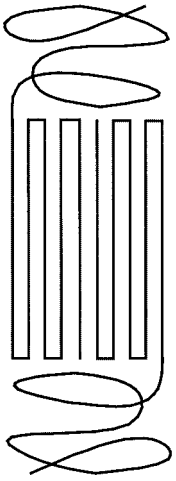

**Figure 1.** Theoretical model proposed for symmetric crystalline/amorphous diblock copolymer.

Although a relatively large body of work exists on crystallizable block copolymers in the bulk, much less work has been done in thin films.[27] Here, we presented a study on thin films of a symmetric poly(ethylene oxide-*b*-1,4-butadiene) (P(EO-*b*-BD)) diblock copolymer. P(EO-*b*-BD) is in the strong segregation limit, yet with a low-$T_g$ amorphous block. The confinement of crystallization arises from the large enthalpic penalty of segmental interactions between the blocks rather than the im-

* To whom all correspondence should be addressed.

10.1021/ma002032c CCC: $20.00 
Published on Web 03/30/2001

mobility of the amorphous block. Nonetheless, the molecular weight of the diblock copolymer is low enough so that the thickness of the lamellar microdomains is much smaller than the thickness of crystals in PEO homopolymers. Each of these characteristics contributes to unusual morphological behavior in thin films of this copolymer.

## Experimental Section

Poly(ethylene oxide-*b*-1,4-butadiene) (P(EO-*b*-BD)) was obtained from Polymer Source. It was synthesized via sequential anionic polymerization where polybutadiene (PBD) was polymerized first. The molecular weights and molecular weight distributions of the PBD block and the entire diblock copolymer were characterized by GPC. The polydispersity of PBD before the addition of ethylene oxide was 1.05. The polydispersity of the final diblock copolymer was 1.04. The molecular weight for the PBD block was 5000 g/mol by using PBD standards. The molecular weight for the PEO block was calculated from $^1$H NMR and was found to be 5500 g/mol. The densities of crystalline and amorphous PEO are 1.13 and 1.03 g/cm$^3$, respectively, while the density of PBD is 0.94 g/cm$^3$. For a high degree of PEO crystallinity, the volume ratio of PEO to PBD in the diblock copolymer is about 1:1. The melting temperature of the PEO block was found to be around 53 °C from DSC measurements.

The thermal stability of P(EO-*b*-BD) was examined by thermogravimetric analysis (TGA). The sample was held at 150 °C in the TGA for 1 h, and no weight loss was observed. GPC results on the material used in this TGA experiment indicated a slight increase of polydispersity to 1.13. The most severe thermal treatment encountered in all of our studies is the melting of the diblock material by holding it at 80 °C for at most 5 min. TGA results indicate that the copolymer is thermally stable under such conditions without noticeable degradation. To avoid absorption of moisture by PEO, samples were dried under vacuum at 50 °C prior to use, and all the samples were stored under vacuum.

Silicon wafers were obtained from International Wafer Service and cleaned according to standard procedures in order to remove adsorbed organic contaminates.[29] The substrates were examined by a Rudolph Research AutoEL-II ellipsometer using a helium−neon laser ($\lambda$ = 632.8 nm) at an incidence angle of 70° and found to be free of organic contaminates. Thin films of P(EO-*b*-BD) were prepared by spin-casting a 2% toluene solution onto a silicon wafer. Films with different thickness can be prepared by changing the concentration of the solution and the spinning speed. The average thickness of the films was characterized by ellipsometry. The diblock copolymer films, on the substrates, were melted at 80 °C for ∼5 min in a Mettler FP80 hot stage. The sample films were subjected to a step change in temperature by quickly transferring them to a second Mettler hot stage preset at the crystallization temperature of interest. The samples were then observed directly with an interference optical microscope. For lower crystallization temperatures (large undercooling) nucleation was fast, whereas for higher crystallization temperatures, nucleation was very slow. Nucleation could be promoted, however, by touching the edge of the wafer with tweezers or by using the self-seeding method described by Kovacs and Gonthier.[30] Experiments at low undercooling can also be conducted by nucleation at a lower temperature followed by a rapid transfer of the sample to another hot stage at a higher temperature.

The structures of the thin films were studied using an Olympus BX60F3 optical microscope. All the optical images were obtained under reflection conditions to obtain interference colors from a white-light source. Normarski conditions were used to enhance the contrast of the terraced surface of the copolymer thin films.[31] The change in birefringence upon crystallization cannot be seen under reflection conditions in the optical microscope. However, crystallization does produce a slight, yet observable, change in the surface topography that enables the study of crystallization in microphase-separated diblock copolymer thin films.

X-ray photoelectron spectroscopy (XPS) was carried out using a Physical Electronics model 5100 with a Mg Kα X-ray source at 500 W. The incident beam angle was 45°, and the sampling depth was about 4 nm.

Silicon nitride ($Si_3N_4$) membranes (100 nm thick) with a window size of 0.46 mm × 0.46 mm were obtained from Structure Probe Inc. A toluene solution of the diblock copolymer was spin-coated onto the membranes. The thin films have the same characteristics as those on silicon wafers as observed via optical microscopy. The polymer thin film was then melted at 80 °C and crystallized at various temperatures. The experimental conditions were exactly the same as those cast on silicon wafers. The silicon nitride membranes permit a direct transmission electron microscope (TEM) observation of and diffraction from thin films.[32] TEM and electron diffraction experiments were performed on a JEOL 2000 FX-II transmission electron microscope. The diffraction camera length was calibrated by using an internal gold standard that was evaporated onto one of the membranes.

## Results and Discussion

**Linear Growth of Crystallites.** Thin films of P(EO-*b*-BD) with an average thickness of 40 nm were spin-coated and then heated to 80 °C. The reflectance optical micrograph shown in Figure 2a shows the distinct color contours across the entire surface of the sample indicative of a microphase-separated morphology with lamellar layers oriented parallel to the wafer.[31] Different colored regions indicate different numbers of layers in an "island and hole" or "terraced" morphology. When this sample was cooled to 25 °C, initially no changes were observed. Subsequently, as seen in Figure 2b, a front, indicated by a change in the topography, was seen moving across the sample. The direction of the front advancement is given by the arrow. The lower magnification image in Figure 2c demonstrates the planar, radial mode of growth associated with the crystallization of PEO block.

The micrographs in Figure 2 show that the terraced surface topography arising from the layered morphology of the copolymer is retained as crystallization proceeds. Consequently, PEO crystallizes within the confined spaces defined by the microphase-separated morphology without disrupting it. As noted, there is a slight color change before and after crystallization, indicating that the film thickness and therefore the lamellar period of the microphase separated structure have changed only slightly upon crystallization at 25 °C. In Figure 2, striations and cracks are visible in the crystallized regions. These result from a combination of the density change upon crystallization of the PEO block and the correspondingly small change in the layer thickness. Laterally constraining the multilayered copolymer morphology to the substrate surface precludes any large-scale lateral contraction of the film during crystallization. Any contraction must occur locally, resulting in crack formation. XPS results (not shown) on the thin films before and after crystallization show that PBD is always located at the polymer−air interface. The thickness of the film measured by AFM was found to be an integral number of lamellar periods. Consequently, PBD must also be located at the polymer−substrate interface.

Crystallizing the diblock copolymer thin film at higher temperatures (lower undercoolings) yields a lower radial growth rate of the crystallization. Optical micrographs of the crystallization front observed at 45 °C are shown in Figure 3. The time interval between parts a and b of

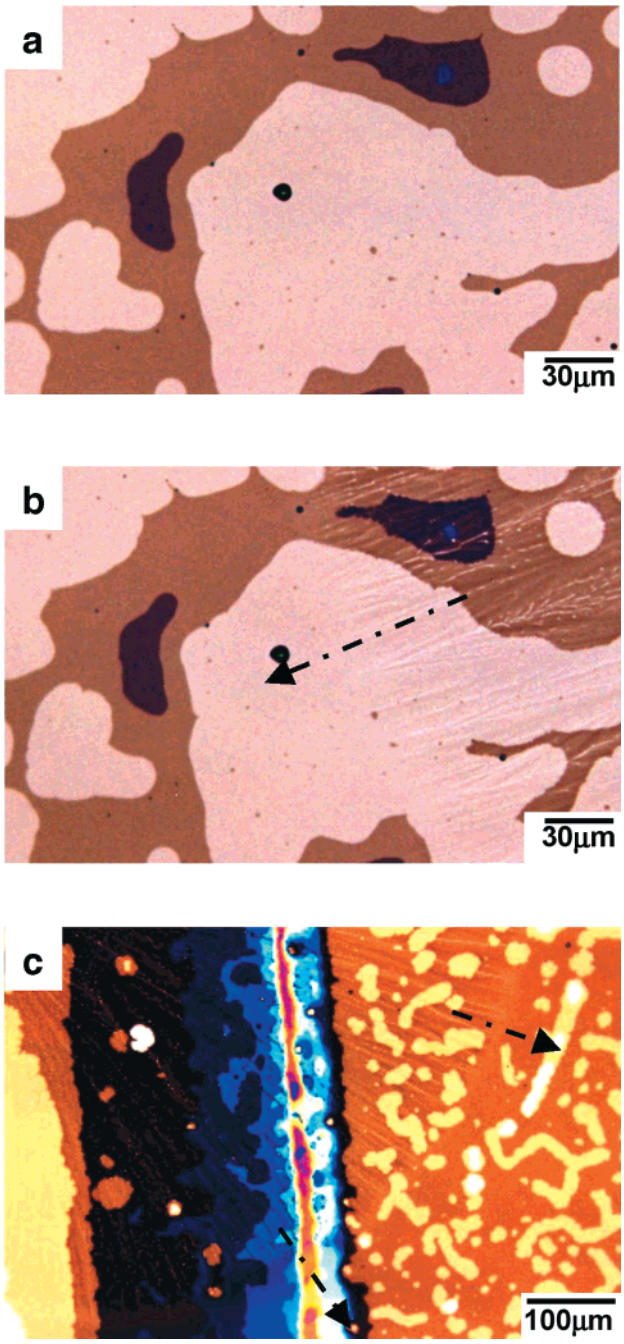


**Figure 2.** Crystallization at 25 °C: (a) thin film at 80 °C; (b) crystallization front at 25 °C; (c) observation at smaller magnification (arrows indicate crystallization directions).

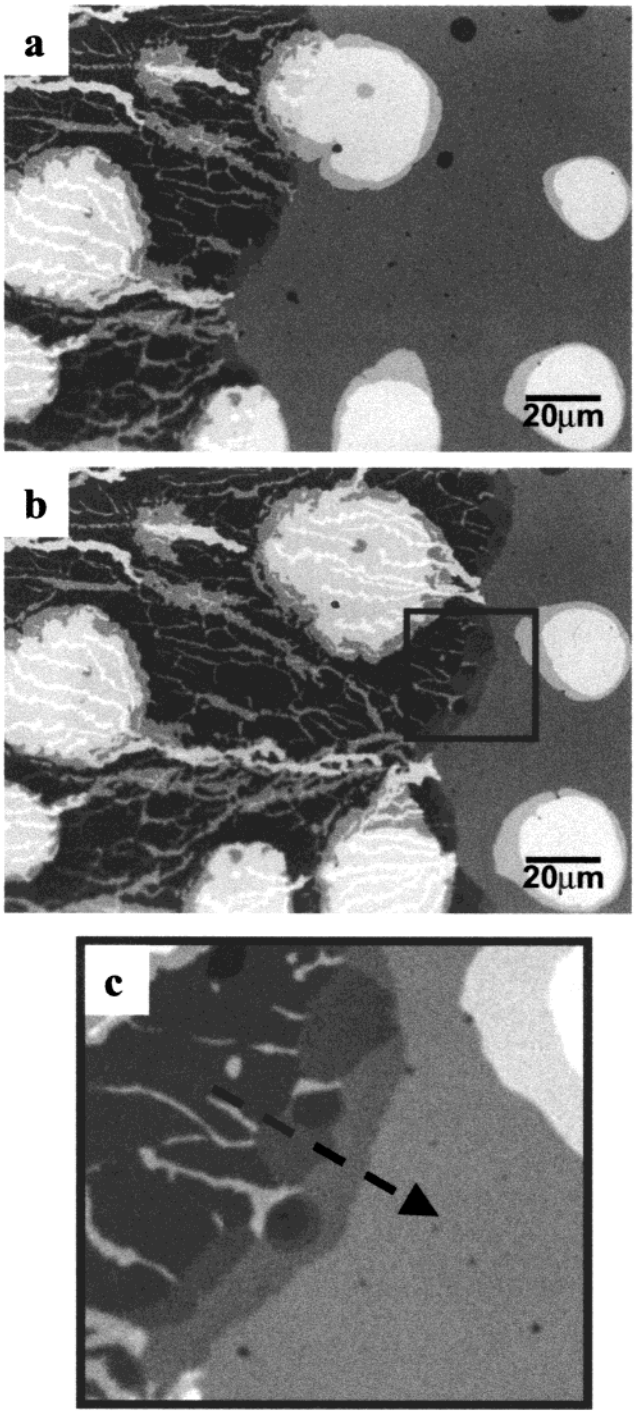


**Figure 3.** Crystallization at 45 °C: (a) earlier time; (b) later time; (c) inset from (b) (arrow indicates crystallization direction).

Figure 3 is only seconds. As seen, the island and hole morphology is still preserved. However, a significant change in the interference colors between the crystallized and molten regions of the film is seen in the micrographs. These color changes correspond to a change in the lamellar period from about 19 to 24 nm brought about by the PEO crystallization. It should be noted that the discrete terracing of the interference colors is still evident after crystallization, showing that crystallization has not destroyed the multilayered structure initially present and has occurred within the layered framework, even though there is a significant increase in the period. However, the extent of cracking in the sample has dramatically increased over that seen at 25 °C. The larger increase in lamellar spacing necessitates a greater lateral contraction in the PEO layers in order to conserve volume. This results in more dramatic cracking.

Figure 3c is an enlargement of the growth front from Figure 3b. These data show that the crystalline growth front proceeds in three separate layers independently as indicated by distinct interference colors, providing direct visual evidence that PEO crystallization proceeds separately in different layers. There are slight differences in the times at which the fronts reach a given position in the film. This type of staggered crystal growth is observed in the spiral overgrowths of chain-folded polymer crystals grown from dilute solution,[33] where the growth in one layer initiates the growth of

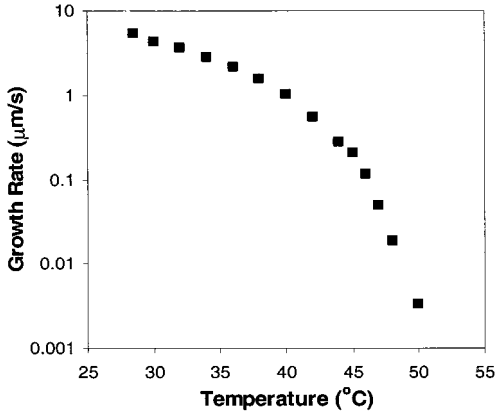


**Figure 4.** Linear crystallite growth rate in thin film.

adjacent layers through a screw dislocation defect.

A careful examination of Figure 3a,b shows another unusual feature of the crystallization within the two-dimensional layered morphology. On the right-hand side of the figures, holes corresponding to film thickness changes are visible. As the crystallization front advances toward these areas, they are strongly distended toward the growth front, even when the growth front is ~10 $\mu$m away! While one would expect transport of PEO chains to the growth front from the fluid phase, the confinement of the crystals within the layered structure along with the large increase in the period results in a substantial lateral contraction causing a distortion of the surface features over very large distances.

The radial growth rate was found to be constant at a given temperature. A plot of this linear growth rate as a function of crystallization temperature is shown in Figure 4. For PEO homopolymers, the temperature dependence of the growth rate is usually discontinuous and can be separated into different regimes due to a change in the integral fold number.[34,35] However, such discontinuities were not observed here over the temperature range studied.

**Self-Seeding Experiments.** When crystallization was conducted at 45 °C or higher, nucleation was very slow and only a few nuclei formed across the entire film. By using a self-seeding method,[30] the number of nuclei increases, and they form more rapidly and at much higher density. In our studies, the sample film was melted by heating to 80 °C for 5 min. It was then quenched to 30 °C and held at this temperature until crystallization was complete. The sample was then heated to 58 °C (slightly higher than the $T_m$ determined by DSC) for 5 min. Figure 5a is an optical micrograph of the thin film at 58 °C where the PEO crystals have melted leaving only a few stable nuclei. Upon cooling to 45 °C, crystallites were found to nucleate at many places in the sample as shown in Figure 5b. As the crystallization proceeds (shown in Figure 5c), the crystallites grow independently in each of the layers. Crystallites growing in the same layer are seen to impinge upon one another. Two crystallites growing in separate, parallel layers appear in the optical micrographs to grow through one another without impinging. The enlarged insets in Figure 5 show these two different cases. These results suggest that nucleation and crystallization can occur independently in different layers.

A series of optical micrographs of a sample film crystallized at 50 °C are shown in Figure 6. The self-

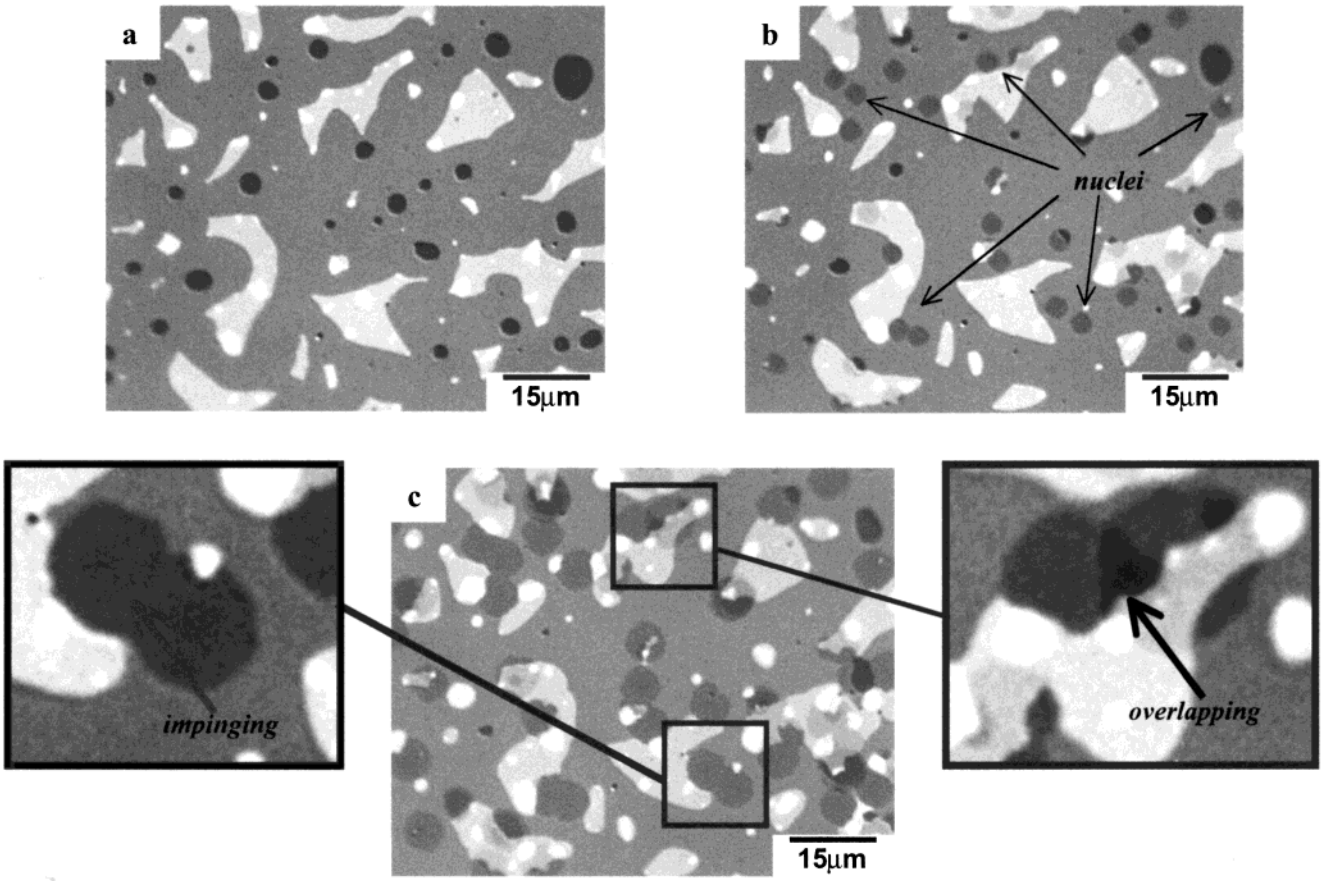


**Figure 5.** Self-seeding crystallization at 45 °C: (a) thin film held at 58 °C; (b) nuclei started to emerge when temperature was lowered; (c) crystallites grew larger and start to impinge or overlap each other.

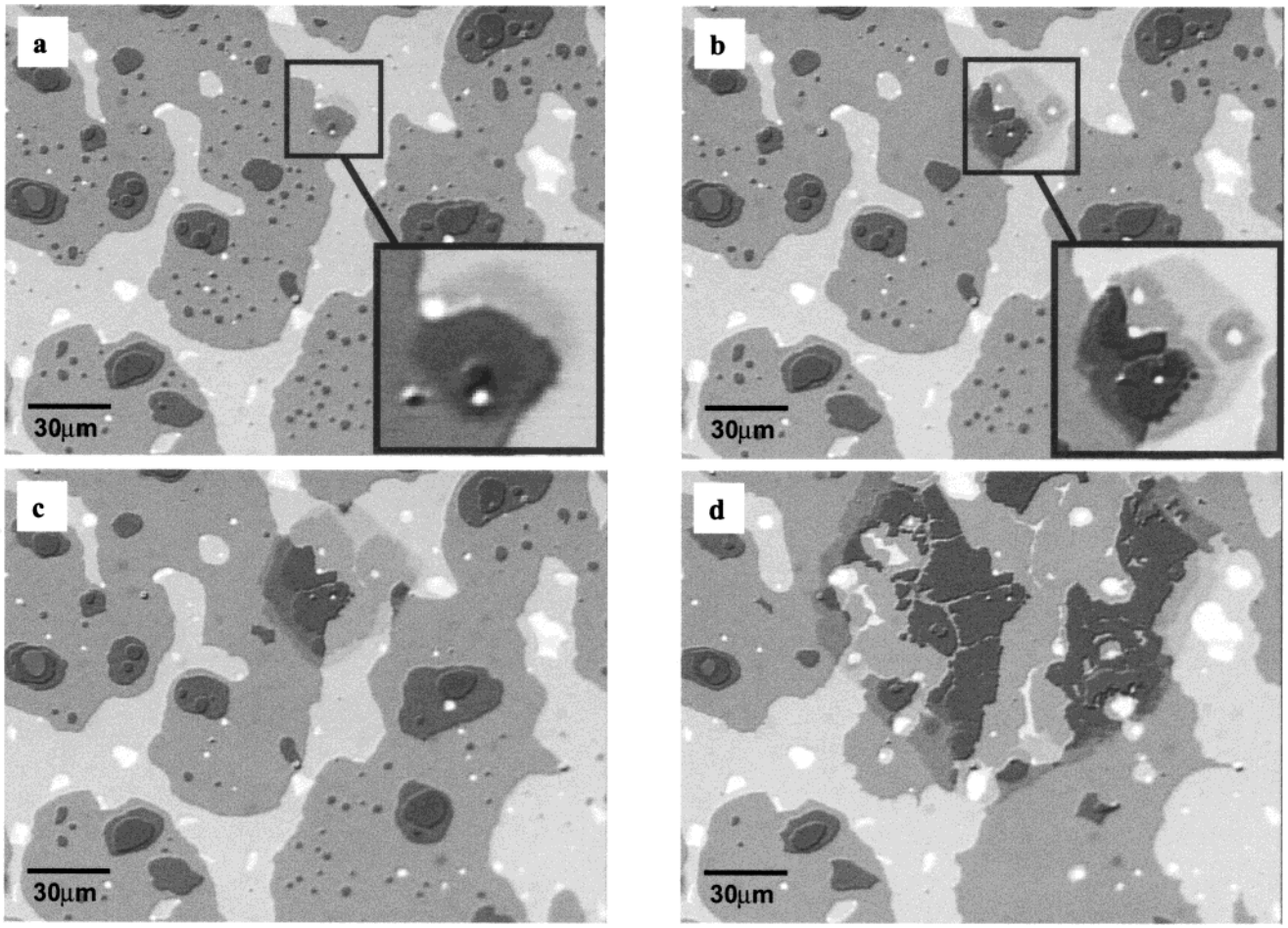


**Figure 6.** Crystal growth and layer propagation at 50 °C: morphology evolution with time.

seeding method was used to ensure fast nucleation. It is most interesting to notice that the growing crystallites adopt a hexagonal shape that resembles the shape of a PEO single crystal.[25,30] The hexagonal shape of the growing crystallite shows little change when the crystallite becomes larger (up to 100 $\mu$m in diameter). Previous observations of PEO single crystals have revealed both square and roughly hexagonal-shaped crystals.[25] We have also observed (not shown) square growth patterns in these diblock thin films. However, in the present study, no attempt was made to distinguish conditions leading to square vs hexagonal crystal habits. Subsequent crystallization of the PEO blocks in adjacent layers was found, leading to what appear to be overgrowths on the original crystallites. The crystallites in different layers propagate "cooperatively" across the sample, which is consistent with the observation of distinct layers in the crystallization front in Figure 3b. The cooperativity of crystallite growth in different PEO layers is suggested by the alignment of crystallite facets, which is particularly evident in Figure 6c. Electron diffraction evidence for cooperative crystallite growth is presented in the next section of this paper. Clearly in this case, the crystalline order in one layer induces the crystallization in adjacent layers, even though the PEO layers are separated by an approximately 100 Å of amorphous PBD.

**Crystalline Chain Orientation.** To further investigate the crystalline structure of PEO blocks, electron diffraction patterns were taken. Diblock copolymer solutions were spin-coated onto silicon nitride membranes that are transparent to the electron beam. The samples were melted at 80 °C and crystallized at various temperatures. The same terraced morphology as that of thin films cast on bare silicon wafers was observed by optical microscopy. Figure 7 shows a low-magnification TEM image of a sample crystallized at 35 °C taken by projecting the electron beam through the silicon nitride membrane and, thus, perpendicular to the microphase-separated layers of PBD and PEO. The island and hole structure is clearly visible from mass thickness contrast arising from the integral number of layers in different areas. The film has, on average, about 6−7 layers of diblock copolymer lamellae on it. Cracking during crystallization has resulted in the small striations on this image. Marked on this image are locations where electron diffraction patterns were taken. The general pattern obtained is a 4-fold spot pattern corresponding to the (120) reflections of PEO. This is identical to the diffraction pattern obtained from PEO single crystals.[25] Numerous diffraction patterns for samples crystallized from 30 to 45 °C were obtained, and all showed the same spot diffraction pattern regardless of the crystallization temperature. The results indicate that PEO chains in the crystal are oriented parallel to the electron beam, and the fold surface plane is normal to the electron beam. Since the microphase-separated layers are oriented parallel to the substrate, the crystalline PEO chain stems are oriented perpendicular to the microphase-separated layers. The results are consistent with the observation of hexagonal-shaped crystalline growth at 50 °C. The morphology of PEO-*b*-PBD thin

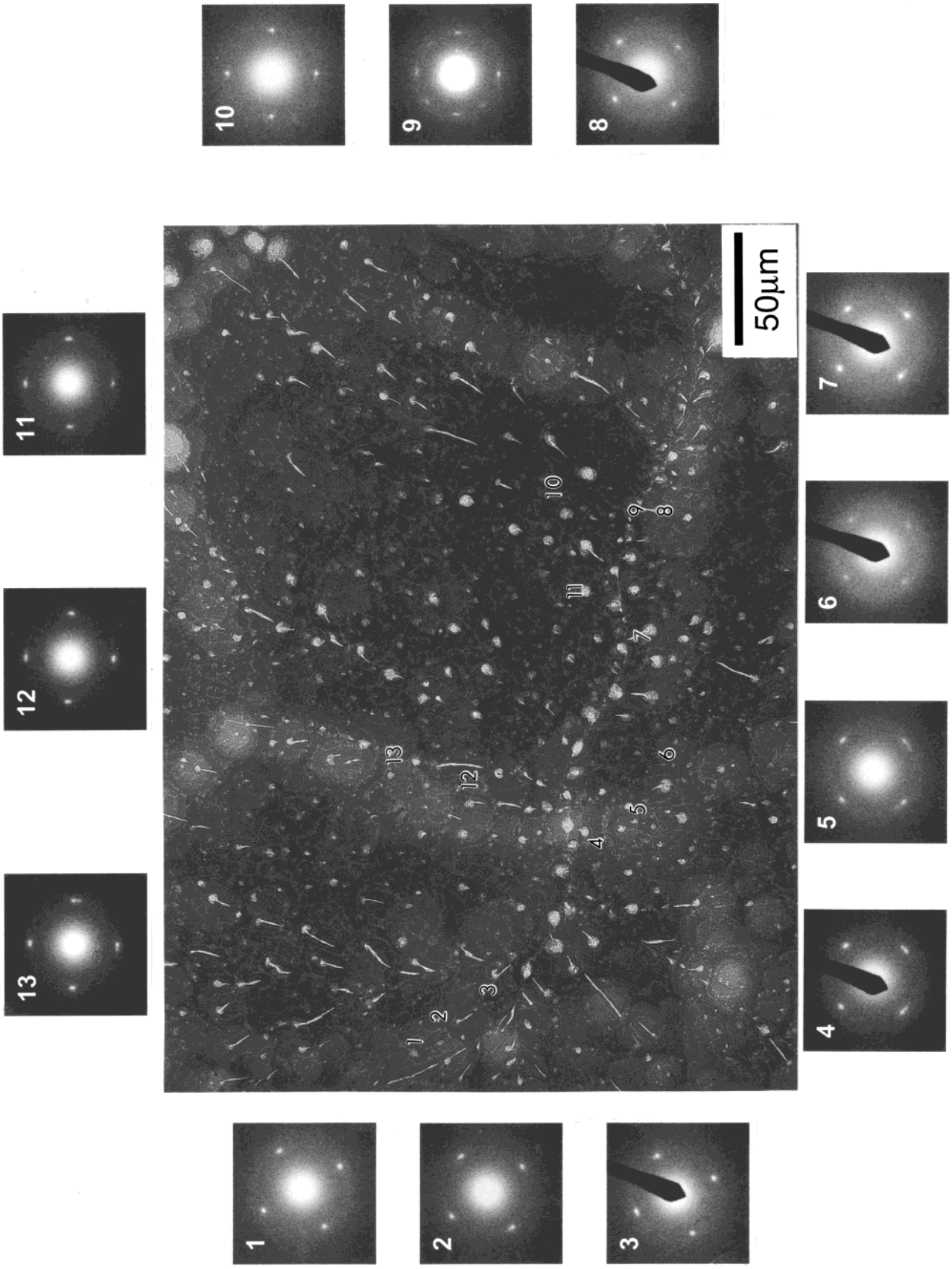


**Figure 7.** TEM image and the electron diffraction patterns showing (120) diffraction from various positions of the film.

films is thus very similar to that proposed theoretically, shown schematically in Figure 1. However, the lamellar long period may not follow the scaling law as predicted by equilibrium arguments and may instead be kinetically controlled. This will be addressed in a future publication.[36]

In electron diffraction patterns 1−8 and 10−12 in Figure 7 only one set of 4-fold spots are observed even though the beam is projecting through multiple layers of the structure and thus multiple crystalline layers of PEO. This can only occur if PEO crystals in adjacent layers are in registry. In the TEM image in Figure 7, there are at least three different sections that are from different nuclei as characterized by straight boundaries among them. The diffraction patterns within these regions (1−3, 4−8, 10−13) have the same (or very similar) crystallographic orientation. Pattern 9 shows eight reflections; however, it was taken at the boundaries between regions where the PEO orientation was different. Consequently, two different oriented regions contribute to this pattern. The eight spot pattern is a result of the overlap of two 4-fold patterns corresponding to the two adjacent regions and is actually a superposition of patterns 8 and 10.

## Conclusions

In the melt, the P(EO-*b*-BD) diblock copolymers form a lamellar morphology oriented parallel to the substrate. Crystallization confined within the microphase-separated PEO layers progresses across the sample with retention of the preformed microphase-separated lamellar morphology. Crystallization at higher temperatures thickens the lamellae but still preserves the layered morphology formed in the melt state. A quantitative analysis of the effect of crystallization temperature on lamellar domain spacing and melting behavior will be reported elsewhere.[36]

The crystallization of one layer was found to induce the crystallization of adjacent layers. The crystallographic registry between adjacent crystalline layers was an unexpected, yet remarkable, result since the crystals are separated by intervening layers of amorphous PBD (∼100 Å thick). This can only occur if the PEO crystallites in adjacent layers originated from the same nucleus and if there is a crystallographic connection between the layers. The development of overgrowth crystallites on a single initial crystallite in Figure 6 supports this conclusion. The facets of the overgrowth crystallites are aligned with those of the parent crystallite. We postulate a defect-controlled mechanism for the spreading of crystallinity between PEO layers. Figure 8a illustrates how an edge dislocation that occurs at the boundary of an island or hole results in the spreading of crystallinity to an adjacent layer. A screw dislocation, as illustrated in Figure 8b, provides a spiral ramp by which crystallinity can spread to many adjacent layers. This screw dislocation mechanism is the same mechanism that leads to overgrowths in solution grown crystallites.[33,37] The difference here is that the screw dislocation is formed in a two-component layered material rather than a single-component material. The structure of screw dislocations in microphase-separated lamellar systems has been discussed by Gido and Thomas.[38] These screw dislocations do not require a discontinuity in the core but rather have the core structure of a helicoid minimal surface. This structure is similar to that of a parking garage in which each

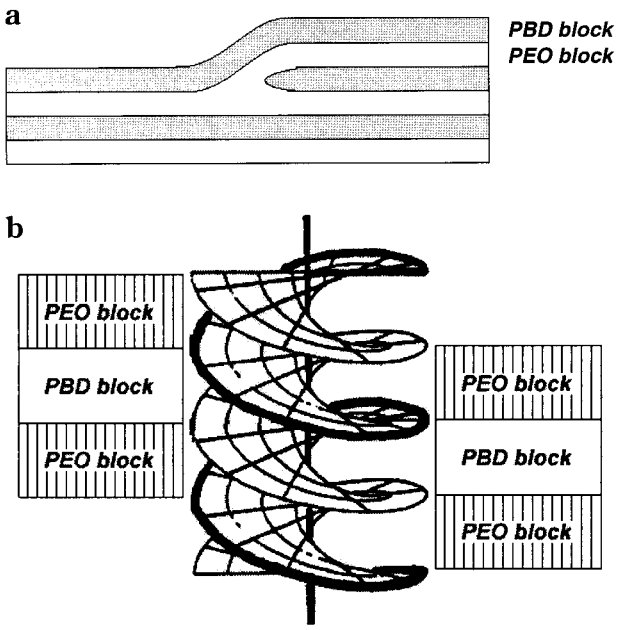


**Figure 8.** Schematics for (a) edge dislocation and (b) screw dislocation.

circuit around the core moves one up or down between adjacent layers of the same type. When a growing crystallite in a single layer encounters this screw dislocation structure, its growth will carry it up and down the screw dislocation and allow it to spread outward in all the adjacent layers. The crystallographic alignment of all these layers follows since the crystallites in all the layers are actually one single crystal connected through the defect. The edge dislocation mechanism also allows for alignment of crystallites in adjacent layers.

**Acknowledgment.** Work at the University of Massachusetts Amherst was supported by the Materials Research Science and Engineering Center (MRSEC) under NSF Grant DMR9809365.

## References and Notes

(1) DiMarzio, E. A.; Guttman, C. M.; Hoffman, J. D. *Macromolecules* **1980**, *13*, 1194.
(2) Whitmore, M. D.; Noolandi, J. *Macromolecules* **1988**, *21*, 1482.
(3) Vilgis, T.; Halperin, A. *Macromolecules* **1991**, *24*, 2090.
(4) Cohen, R. E.; Cheng, P. L.; Douzinas, K.; Kofinas, P.; Berney, C. V. *Macromolecules* **1990**, *23*, 324.
(5) Douzinas, K. C.; Cohen, R. E.; Halasa, A. F. *Macromolecules* **1991**, *24*, 4457.
(6) Hamley, I. W.; Fairclough, J. P. A.; Bates, F. S.; Ryan, A. J. *Polymer* **1998**, *39*, 1429.
(7) Khandpur, A. K.; Macosko, C. W.; Bates, F. S. *J. Polym. Sci., Polym. Phys. Ed.* **1995**, *33*, 247.
(8) Kofinas, P.; Cohen, R. E. *Macromolecules* **1994**, *27*, 3002.
(9) Sakurai, K.; MacKnight, W. J.; Lohse, D. J.; Schulz, D. N.; Sissano, J. A.; Lin, J. S.; Agamalyan, M. *Polymer* **1996**, *37*, 4443.
(10) Quiram, D. J.; Register, R. A.; Marchand, G. R.; Adamson, D. H. *Macromolecules* **1998**, *31*, 4891.
(11) Rangarajan, P.; Haisch, C. F.; Register, R. A.; Adamson, D. H.; Fetters, L. J. *Macromolecules* **1997**, *30*, 494.
(12) Loo, Y. L.; Register, R. A.; Ryan, A. J. *Phys. Rev. Lett.* **2000**, *84*, 4120.
(13) Park, C.; De Rosa, C.; Fetters, L. J.; Thomas, E. L. *Macromolecules* **2000**, *33*, 7931.
(14) Gast, A. P.; Vinson, P. K.; Cogan-Farinas, K. A. *Macromolecules* **1993**, *26*, 1774.
(15) Gervais, M.; Gallot, B. *Makromol. Chem.* **1973**, *174*, 193.

(16) Mai, S.; Fairclough, J. P. A.; Hamley, I. W.; Matsen, M. W.; Denny, R. C.; Liao, B.; Booth, C.; Ryan, A. J. *Macromolecules* **1997**, *30*, 8392.
(17) Ryan, A. J.; Hamley, I. W.; Bras, W.; Bates, F. S. *Macromolecules* **1995**, *28*, 3860.
(18) Ryan, A. J.; Fairclough, J. P. A.; Hamley, I. W.; Mai, S.; Booth, C. *Macromolecules* **1997**, *30*, 1723.
(19) Zhu, L.; Cheng, S. Z. D.; Calhoun, B. H.; Ge, Q.; Quirk, R. P.; Thomas, E. L.; Hsiao, B. S.; Yeh, F. J.; Lotz, B. *J. Am. Chem. Soc.* **2000**, *122*, 5957.
(20) Zhu, L.; Chen, Y.; Zhang, A.; Calhoun, B. H.; Chun, M.; Quirk, R. P.; Cheng, S. Z. D.; Hsiao, B. S.; Yeh, F.; Hashimoto, T. *Phys. Rev. B* **1999**, *60*, 10022.
(21) Nojima, S.; Kato, K.; Yamamoto, S.; Ashida, T. *Macromolecules* **1992**, *25*, 2237.
(22) Ishikawa, S.; Ishizu, K.; Fukutomi, T. *Eur. Polym. J.* **1992**, *28*, 1219.
(23) Liu, L.-Z.; Yeh, F.; Chu, B. *Macromolecules* **1996**, *29*, 5336.
(24) Lotz, B.; Kovacs, A. J. *Kolloid Z. Z. Polym.* **1966**, *209*, 97.
(25) Lotz, B.; Kovacs, A. J.; Bassett, G. A.; Keller, A. *Kolloid Z. Z. Polym.* **1966**, *209*, 115.
(26) Gervais, M.; Gallot, B. *Makromol. Chem.* **1973**, *171*, 157.
(27) Hamley, I. W.; Wallwork, M. L.; Smith, D. A.; Fairclough, J. P. A.; Ryan, A. J.; Mai, S.-M.; Yang, Y.-W.; Booth, C. *Polymer* **1998**, *39*, 3321.
(28) Mai, S.; Fairclough, J. P. A.; Hamley, I. W.; Matsen, M. W.; Denny, R. C.; Liao, B.; Booth, C.; Ryan, A. J. *Macromolecules* **1996**, *29*, 6212.
(29) Fadeev, A. Y.; McCarthy, T. J. *Langmuir* **1999**, *15*, 3759.
(30) Kovacs, A. J.; Gonthier, A. *Kolloid Z. Z. Polym.* **1972**, *250*, 530.
(31) Coulon, G.; Russell, T. P.; Deline, V. R.; Green, P. F. *Macromolecules* **1989**, *22*, 2581.
(32) Morkved, T. L.; Lu, M.; Urbas, A. M.; Ehrichs, E. E.; Jaeger, H. M.; Mansky, P.; Russell, T. P. *Science* **1996**, *273*, 931.
(33) Keith, H. D.; Padden, F. J. *J. Appl. Phys.* **1964**, *35*, 1286.
(34) Kovacs, A. J.; Gonthier, A.; Straupe, C. *J. Polym. Sci., Polym. Symp.* **1975**, *50*, 283.
(35) Kovacs, A. J.; Straupe, C.; Gonthier, A. *J. Polym. Sci., Polym. Symp.* **1977**, *59*, 31.
(36) Hong, S.; MacKnight, W. J.; Russell, T. P.; Gido, S. P. Manuscript in preparation.
(37) Khoury, F.; Passaglia, E. In *Treatie on Solid State Chemistry;* Plenum: New York, 1976; Chapter 6.
(38) Gido, S. P.; Gunther, J.; Thomas, E. L.; Hoffman, D. *Macromolecules* **1993**, *26*, 4506.

MA002032C